DOI: https://doi.org/10.53040/cga12.11 UDC: 616-056.7:577.344

GENERATION OF PHOTONIC MOLECULAR COMPLEXES UNDER THE ACTION OF ULTRAVIOLET LIGHT IN THE DNA/RNA INACTIVATION PROCESS

Diana PODOLEANU, ORCID 0009-0006-9087-6445
Ion MUNTEANU, ORCID 0000-0002-5685-8888
Elena STARODUB, ORCID 0009-0006-5621-8123
Gheorghe CHIRMAN
Nicolae ENAKI, ORCID 0000-0002-4571-7457
enache_nicolae@yahoo.com

Quantum Optics and Kinetic Process Lab., Institute of Applied Physics of Moldova State University, Chisinau, Republic of Moldova

Abstract. A semi-classical model (classical by the field and quantum by describing biomolecules) is proposed, which establishes the dependence of the DNA/RNA dimerization rate on ultraviolet C (UVC) radiation intensity. In particular, a nonlinear model based on cooperative processes similar to the Raman-like in quantum optics is developed. The main result of the theory demonstrates that the dimerization process in DNA/RNA strongly depends on the UVC light intensity, thus proving a possible quantum microscopic mechanism of UVC light interactions with DNA. A notion of a photonic molecule consisting of the normal state and the dimer state under the action of the bimodal Raman field is given. This type of molecule exists only in the presence of the excited field, and after it is turned off, the biomolecule remains part of the time in the entangled state after which DNA dimerization is probabilistically established. A nonlinear dependence on the intensity of the applied radiation was established, which was confirmed in a series of experiments on the inactivation of pathogens (or yeast colonies) reproduction under the action of ultraviolet radiation. The main objective of this study was to establish a link between the intensity of UV C radiation and the efficiency of decontamination using metamaterials with an increased contact surface with contaminated fluid by pathogens, that cause nosocomial infections, namely Escherichia coli, Pseudomonas aeruginosa, Candida albicans, and Candida glabrata. These microorganisms were put through different forms of packing, both thick fibers repacked with thin fibers and millimeter balls repacked with sub-millimeter quartz balls. The results demonstrate that bacterial pathogens respond differently to exposure to UV-C radiation, depending on the contact surface created between the elements of the quasi-periodic metamaterials.

Keywords: raman conversion, cooperative dimerization, critical intensity for dimerization, metamaterials in inactivation, photonic biomolecules.

INTRODUCTION

The possibility of creating localized states linked between cellular partners was an idea proposed by Kasha and is actually the basis of the formation of some supracellular structures in which the excited state is relatively stable in time and the electronic subsystem does not recombine in time. Such supracellular patterns could arise upon the

cooperative absorption of photons in the multiple Raman scattering process. This model assumes that between the normal state and the excited state of the bipolar molecules it is possible to form a localized state of the electrons of both molecules so that the system has a relatively long lifetime. If we talk about a system of such bipolar molecules upon excitation, they can enter into a bipolar bond that could lead to the formation of relatively large molecules. A model of multiple excitation of molecular states and the formation of molecular clusters in induced Raman scattering is proposed in this chapter. The model is reduced to the multiple steps of absorption and emission of photons in the scattering process. The model could be used in photosynthesize using natural and artificial photoreceptors, mostly of microbial origin, to be genetically introduced into the cells of interest. For the multiple Raman effect to have an increased efficiency, optical cavities are needed. In biological systems, such optical cavities are observed. For example, in photosynthesis, both the chloroplast membrane and its internal elements are used as a resonator. The chloroplast is a structure in the cells of plants and green algae that is the site of photosynthesis, the process by which light energy is converted into chemical energy, resulting in the production of oxygen and energy-rich organic compounds. With the introduction of photosensitive opsin/rhodopsin it was observed that cells that are naturally insensitive to light can be made photosensitive and addressable by illumination and can be precisely controlled in time and space. If we look at some proteins as radiation accumulation resonators, then possibilities of selective Raman directing when introducing such proteins into the cell can take place at the subcellular level. In other words, the cellular subsystems are activated by applying control elements such as promoters, enhancers and specific targeting sequences to the DNA/proteins encoding the photoreceptor used. This powerful approach enables precise characterization and manipulation of cellular functions and has motivated the development of advanced optical methods for patterned photostimulation.

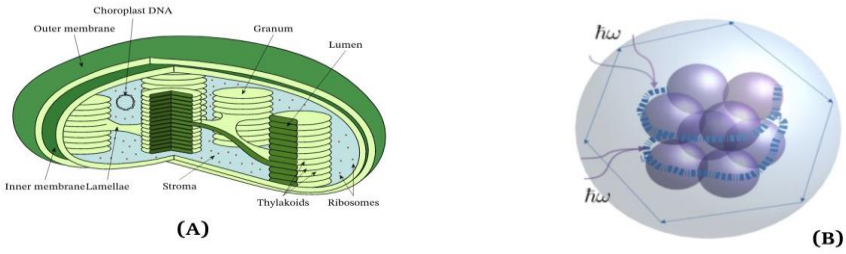


Figure 1. (A) Observation of disc-shaped optical microresonators (photore- ceptors) in chloroplasts in the process of storing and using radiation in photosynthesis. (B) Observation of spherical Hystone elements in the DNA packing [1, 2, 3, 4, 5].

As follows from the literature [1, 2] a nucleosome is the basic structural unit of DNA packaging in eukaryotes and may serves not only support for DNA cain

but the possible electro- magnetic contact through the evanescent zone of the elements of this repached structure in nucleus with dimension about 5- 10 micrometers. The structure of a nucleosome consists of a segment of DNA wound around eight histone proteins [1, 2] and resembles thread wrapped around a spool. The nucleosome is the fundamental subunit of chromatin. Each nucleosome is composed of a little less than two turns of DNA wrapped around a set of eight proteins called histones, which are known as a histone octamer. Each histone octamer is composed of two copies each of the histone proteins H2A, H2B, H3, and H4 (see Ref. [3, 4, 5]). Due to the fact that the refractive index of histone elements is higer than the water one it is posible to brelize the standung or guide waves in such a system like in the traditional optical emements Ref.

In ADN modification, the histones are highly basic proteins abundant in lysine and arginine residues that are found in eukaryotic cell nuclei and play an imortant role in the localization of vibration waves as this take place in microspherical resonators (see Fig. 1) B. They act as spools around which DNA winds to create structural units called nucleosomes [3, 4]. Nucleosomes in turn are wrapped into 30-nanometer fibers that form tightly packed chromatin. Histones prevent DNA from becoming tangled and protect it from DNA damage. In addition, histones play important roles in gene regulation and DNA replication. Without histones, unwound DNA in chromosomes would be very long. For example, each human cell has about 1.8 meters of DNA if completely stretched out; however, when wound about histones, this length is reduced to about 90 micrometers (0.09 mm) of 30 nm diameter chromatin fibers [5]. In other words, the subsystems of the cell nucleus in eukaryotes are activated by applying control elements, such as promoters, enhancers and specific targeting sequences, to the DNA/proteins that encode the photoreceptor used. This powerful approach enables precise characterization and manipulation of cellular functions and has motivated the development of advanced optical methods for patterned photostimulation. A huge catalogue of histone modifications have been described, but a functional understanding of most is still lacking. Collectively, it is thought that histone modifications may underlie a histone code, whereby combinations of histone modifications have specific meanings. However, most functional data concerns individual prominent histone modifications that are biochemically amenable to detailed study.

Modification of Biomolecular Structural Changes Under UVC Radiation

Experimental results: analyses of dynamical and static regime The core of the equipment proposed in the Refs. [6, 7, 8] was adapted to the new conception of the repacking of studied metamaterial small quartz balls/fibers between the big one. Taking into consideration that numerous pathogens are more sensitive to UVC radiation than eukaryotic cellular structures, we had to substitute these

contaminated dangerous fluids with yeast solution, the DNA of which has larger resistance to UVC radiation in comparison with many viruses or bacteria. In comparison with Ref.[7], where the yeast solution was inactivated after 10 − 15 min, in this investigation the fungal solution was decontaminated after 24 hours of the preparation moment. We suggested inactivating the yeast fungus as a function of exposition time and the applied intensity of UVC radiation. The inactivation ate this yeast fungal solution depends on the tunnelling effect between normal and dimerized DNA states described in the Ref [6]. The measurements were done after 10 and 20 min of inactivation in the dynamic regime (see Figs. 2).

The consecutive action of 6 lamps on the yeast solution during 10 and 20 minutes time duration: Figures (a) represent the preparation of yeast fungal solution before going through the decontamination system for 6 experiments, which contain from one to 6 active UVC lamps; Figures (b) describe the yeast fungus after it has gone through decontamination system about 10 min for 6 experiments in which the lamps were switched off from one to 6 lamps consecutively. Figures (c) correspond to 20 min inactivation time in the same consecutive application of external intensity of UVC sources. This gives us the possibility to find the dependence of the decontamination rate as the function of the intensity of applied UVC radiation in the lamp units. The mediation in the number and dimensions of colonies observed in the 20 experiments, in which of it was observed about 750-800 fungal colonies per figure. Our decontamination core with 0.8 meters length and 2.5 cm in diameter are filled up with a diameter of spheres about 0.5 − 1 mm of the quartz material. The core is covered by 6 mercurial lamps, which a maximum of radiation is 250 − 260 nm. To improve the efficiency of UVCradiation, all the system is placed in an aluminum cylinder with a diameter of about 20 cm so that the intensity of the radiation in the center of the big cylinder increase significantly due to the reflection proprieties of the aluminum. More than this, the researchers and people in the room are well protected from the direct action of UVC radiation obtained from 6 lamps represented in the Figs. 2.

The initial prepared yeast solution. These figures were obtained by multiple testes by the microscope after 24 hours of the prepared yeast solution. We have prepared the yeast solution, dissolving 25 g of fungal yeast into 800 g of water. In order to improve the development of fungi, we add 20 g of agar, $C_{14}H_{24}O_9$. At the initial stage of the development of fungi, we observed the appearance of various numbers of yeast fungus colonies with aleatory dimensions. Such an experiment with the inactivation of fungal colonies in the earlier time development interval of about 15 min (See Refs [6, 7, 8]).

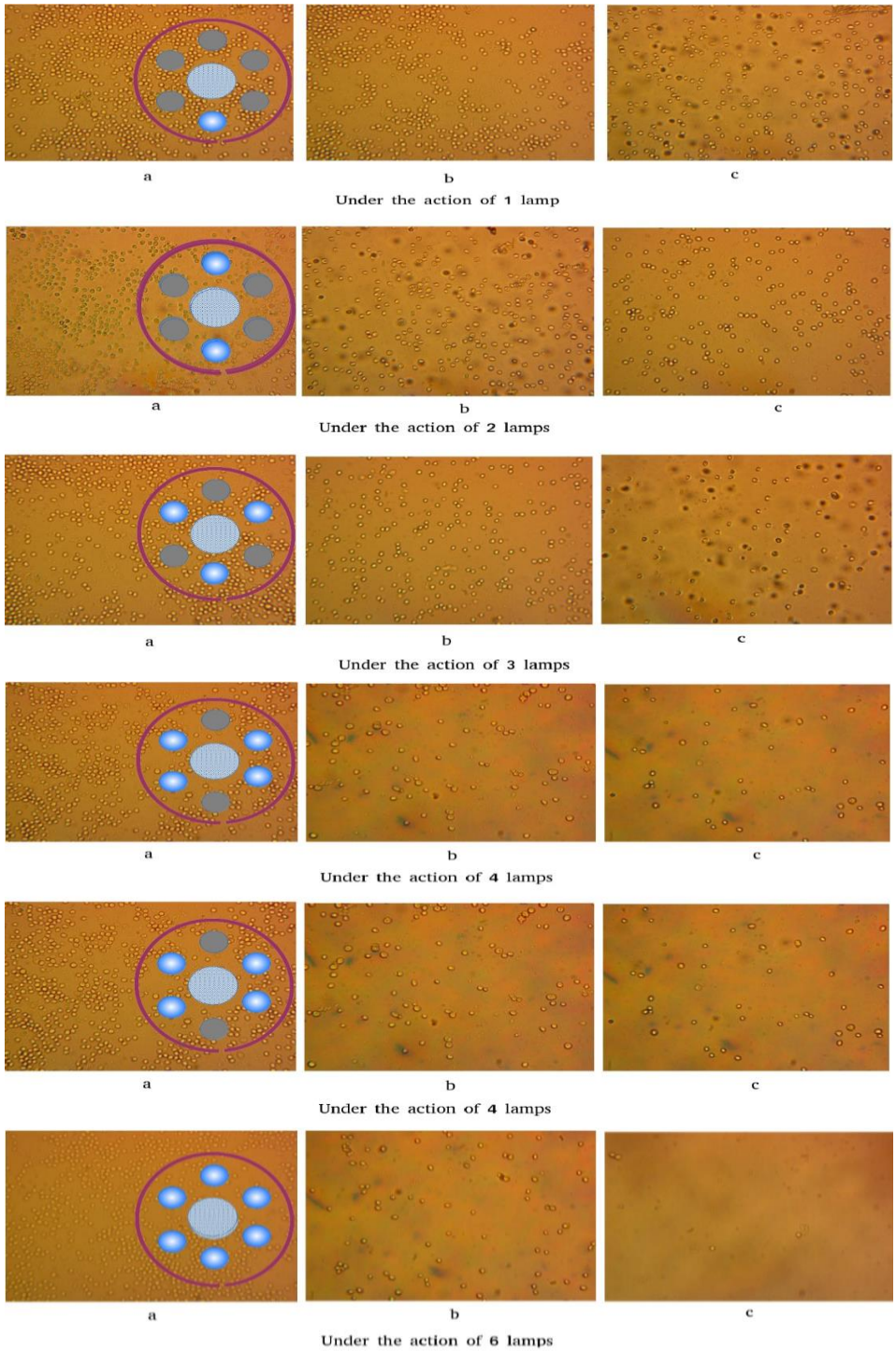


Figure 2. Dynamic regime of decontamination*.

*Figure 2. Dynamic regime of decontamination. *The consecutive action of 6 lamps on the yeast solution during 10 and 20 minutes time duration: Figures (a) represent the preparation of yeast fungal solution before going through the decontamination system for 6 experiments, which contain from one to 6 active UVC lamps; Figures (b) describe the yeast fungus after it has gone through decontamination system about 10 min for 6 experiments in which the lamps were switched off from one to 6 lamps consecutively. Figures (c) correspond to 20 min inactivation time in the same consecutive application of external intensity of UVC sources. This gives us the possibility to find the dependence of the decontamination rate as the function of the intensity of applied UVC radiation in the lamp units. The mediation in the number and dimensions of colonies observed in the 20 experiments, in which of it was observed about 750 - 800 fungal colonies per figure.*

As the development of fungal colonies have some quick developments and some parameters slightly fluctuate in time, we decided to put the inactivation experiments after 24 hours before going through the decontamination equipment. In this experiment, we take into consideration the acceleration of fungal colonies and the intensity dependence of the inactivation rate of yeast fungi by consecutive adding from one to six UVC lamps inside the yeast decontamination core represented in Fig.2.

The first experimental mechanism is connected to improving the contact surface between UVC radiation and contaminated fluid. As we know, the direct radiation on the open surface of non-transparent fluid can not give us the expected result in this area due to the small penetration distance of applied UVC radiation. If we introduce into translucent infected fluid elements of connected quarts metamaterials consisting of optical fibers/spherical elements, we can observe that the total contact surface consists of the surface of each element multiplied by their number. This effect gives us increased decontamination volume, which may be estimated by multiplying the total contact surface of metamaterial elements multiplied by the penetration deep of UVC radiation into the fluid.

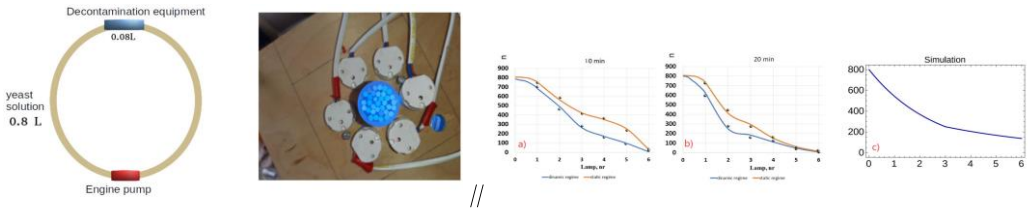


Figure 3. Decontamination speed obtained with left-hand equipment according to the applied intensity of UVC radiation in units of number of lamps:
a) 10 Min dynamic and static regimes; b) 20 Min dynamic and static regimes; c) The dependence of the inactivation rate according to the intensity applied typically in accordance with the proposed theoretical model.

The construction and non-uniform arrangement of optical elements of quasi periodic structures create rotation canals for pathogens or infected aerosols from

the fluid. So, during the rotation, as a function of flow velocity, the infected quasi particles or pathogens suffer deposition on the evanescent zone of each element of metamaterial penetrated by UVC radiation, due to the fact that their density is larger than the fluid one. The last acceleration mechanism depends on the fluid velocity stimulated by the pump engine. This pump mechanism generates the rotation of pathogens/droplets around elements of the metamaterial inducing an inertial force to them so that these particles are deposed on the surface of each element of the metamaterial, where the intensity of UVC radiation is significantly larger than between the elements. On the basis of these two effects in our laboratory was elaborate two equipment for the decontamination of infected liquids and gases (see Figs. 3 and). Experiments have conclusively demonstrated that both quartz spheres and optical fiber metamaterials can effectively annihilate Coliform (including Escherichia coli), or Enterococcus bacteria, as well as yeast and Kombucha cultures.

Physical Model of Nonlinear Photo-transformation and Dimerization of Biomolecules

The Raman model demonstrates that the dimerization rate of thymine bases (T = T) increases exponentially with the intensity of UVC radiation, suggesting the involvement of a quantum mechanism in dimer formation. This process has been experimentally confirmed through resonant fluorescence techniques, which highlight the disruption of hydrogen bonds and associated structural transitions.

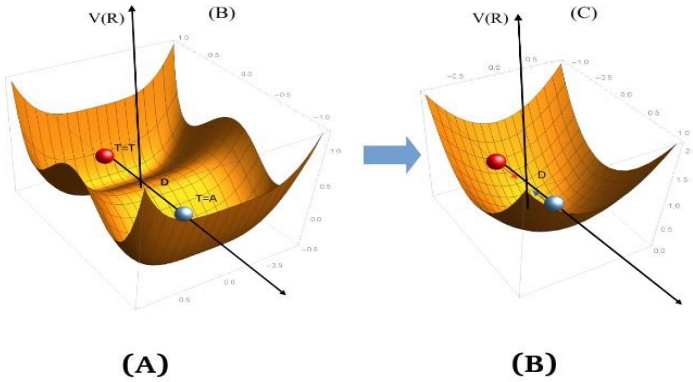


Figure 4. The transition from double well potential
(A) to single well potential (B) when the UVC field strength increases to a critical value I_c.

For the description of the intensity dependence of the modification of the DNA structure under the action of UVC radiation, we propose the Born-Oppenheimer (BO) frequently used in chemistry and microbiology. In this approach, the nuclei subsystem is characterized by the vectors, R1, R2...Rn , and is

considered a slow subsystem compared to the electronic one, r = {r1,r2...rn}. This allows us to represent the molecular wave function by the product of the wave functions, $|\Psi e(r,R)\rangle|\chi(R)\rangle$, of the subsystems of electrons, $|\Psi e(r,R)\rangle$, and the subsystem of nuclei, $|\chi(R)\rangle$, of the respective molecules: . The modification of DNA and RNA structures takes place under the action of UVC radiation, as schematically represented in Fig.2 A by modification of covalent bonds, and in figures 2 A,B by changes in interaction potential. Considering that the nuclei positions are fixed for electronic subsystem the Schrodinger equation can be represented in the form $He(r,Rs)|\Psi e(r,Rs)\rangle = Ee(Rs)|\Psi e(r,Rs)\rangle$. Obviously, the electronic energy eigenvalue Ee depends on the chosen positions R of the nuclei. Varying these positions R in small steps and repeatedly solving the electronic Schrodinger equation, one obtains Ee(Rs) as a function of Rs. We start with DNA dimer modification of the near nucleotide bonds under the action of electromagnetic field. The interaction energy of molecular electrical multi-poles may be approximated with the work of the electrical field during the displacements of electron at distance rj , HI = − ejU(rj), neglecting the magnetic part of the field, where U = rj 0 ($d\vec{r}$, $\vec{E}(\vec{r})$) [19].

For the construction of the possible molecular states till and after the action of UVC radiation we propose to represent the covalent bounds of the two steps of nucleobases in DNA [20, 17]. In the formation of covalent bonds, electron orbitals overlap in order to form molecular orbitals, which give us the simplest prototype of molecules with covalent bonds observed in the H2 molecule in the archetypal Lewis pair $|\Psi(H2;\zeta,R)\rangle = [2(1 + Sab)]^{-1/2}[|\varphi a(1)\rangle|\varphi b(2)\rangle+|\varphi b(1)\rangle|\varphi a(2)\rangle]$,where we involve the overlap integral Sab , defined as, $Sab = \varphi a(r)\varphi b(r)dr$, is dependent on the orbital exponent, ζ ,and the inter-nuclear separation R . It is considered that in covalent bound take place two electrons a and b.

$$H^{(n)} = -\frac{\hbar^2}{2M}\Delta_R + \frac{M\Omega_u^2(R-Q_0)^2 + M\Omega_d^2(R-D_0-\Theta_0)^2}{2} - \frac{2(I\alpha)^2 + 2(I\beta)^2}{M\Omega^2} + \Delta V(R) + \mathcal{E}_0(R_0).$$

So, one may conclude that as a function of intensity of the applied field, the potentials can overlap each other. This effect we name the formation of one photon molecula under the action of external coherent field. We point out that in Fig. 4 the first potential corresponds to the normal state of thymine and the second one corresponds to the dimer state and as function of intensity these two states can collapse in one. In the absence of the UVC these states are separated (D0 > |Q|). According to this situation, the thymine nuclei rings are in one of the Fock states, $|n\rangle u$ or $|n\rangle d$. The first eigenvector corresponds to the solution of the oscillator

equation, (− ¯h2ΔQ/(2M) + MΩ2Q2/2)|n⟩u= ¯hΩu(n + 0.5)|n⟩u, and the second corresponds to possible pyrimidine dimerization of DNA/RNA after the action of the electromagnetic field, (−¯h2ΔΘ/(2M)+MΩ2Θ2/2)|n⟩d= ¯hΩd(n+0.5)|n⟩d. Now, there could appear a question like: For which intensity of the applied field these two states may become mixed? Looking to the Hamiltonian (1), we observe that in the harmonic approximation two oscillation points may coincide, i.e. R − Q0 = R − D0 − Θ0. This corresponds to the situation in which D0 = Q0−Θ0, see the overlap of two minima in the double-well potential, represented in Fig. 4. In this case the field may act on the carbon rings positions of two adjacent thymine nucleotides (or uracil in RNA strand) in anti-phase, so that the oscillation positions of both protonated bonds between two pyrimidines in the normal and dimer states coincide. In this special case, we also simplify the nuclei Hamiltonian (1), reducing it to the harmonic form ˆ H(n) = −¯hΔ2 R/(2M) + (MΩ2 u + MΩ2 d)(R − Q0)2/2. The stationary solution of this entangled state of the two bonds is found from the Schrodinger equation, ˆ H(n)|n⟩ = ¯h Ω2 u +Ω2 d(n + 1/2)|n⟩. After the decoupling of the external UVC field, this common state is decoupled at distance, D0, and becomes proportional to the sum of the two states, |n⟩ ∼ c1|n⟩d+c2|n⟩u, where c2 1+c2 2 = 1. This process corresponds to the dimerization of DNA/RNA nucleotides. The main problem corresponds to the estimation of the critical intensity of UVC field, Ic = D0/(ku − kd), from which follows that ku − kd > 0, and this is possible when the both expressions, ∂Π(0)/∂Q and ∂Π(0)/∂Θ, have opposite signs. With the decreasing of the intensity of the applied field the value of Θ0(I) slightly differs from Q0(I) when considered in the definition of D0 = Θ0(Ic) − Q0(Ic). According to the perturbation theory, in this case the coordinates of these oscillators may be replaced by the expressions:

R−Q0(Ic)+ΔQ0(I)andR−D0+Θ0(Ic)+ΔΘ0(I),whereΔQ0(I) = 2(Ic−I)α/(MΩ2 u), ΔΘ0(I) = 2(Ic−I)β/(MΩ2 d). As result, the perturbed potential shows the attenuation of the tunneling effect with the decreasing of the intensity of the applied UVC field.

DISCUSSION AND CONCLUSIONS

We conclude that by increasing the intensity of the applied radiation in a fixed time interval, the number of yeast colonies decreases nonlinearly up to a given intensity and after, a slow linear decreasing prevails. This result confirms the theoretical prediction. Particularly, by taking into consideration the conclusions of the perturbation theory, the intensity dependence of the overlapping of the wave functions in the double-well potential can be applied to this experiment. We may consider the efficiency of the tunneling effect between normal and dimerized DNA states proportional to the shifts defined in the theory as ΔQ0(I) = 2(Ic − I)α/(MΩ2 u) and ΔΘ0(I) = 2(Ic − I)β/(MΩ2 d), so the effect correlates the experimental result

obtained from Eq. 1. Therefore, one finds a phenomenological correlation between the experimental observations of yeast inactivation dependent on the intensity of irradiation and the theoretical framework explaining the process of dimerization of yeast's DNA by the UVC irradiation. The decontamination parameter of the system becomes proportional to the compression of the double-well potential and the tunneling of the electrons between two stationary states increases as a function of the intensity of the irradiation.

Acknowledgments: This paper was financially supported by the Moldova State University Grant for Institute of Applied Physics (2024 - 2027), and State Project 24.80012.5007.26SE: Stimulating excellence in research for the years 2024-2025.

REFERENCES

1. Reece J., Campbell N. (2006). Biology. San Francisco: Benjamin Cummings. ISBN 978-0-8053-6624-2.
2. Alberts B. (2002). Chromosomal DNA and Its Packaging in the Chromatin Fiber. In Molecular biology of the cell (4th ed.). New York: Garland Science. p. 207. ISBN 978-0-8153-4072-0.
3. Youngson R.M. (2006). Collins Dictionary of Human Biology. Glasgow: HarperCollins. ISBN 978-0-00722134-9.
4. Cox M., Nelson D.R., Lehninger A.L. (2005). Lehninger Principles of Biochemistry. San Francisco: W.H. Freeman. ISBN 978-0-7167-4339-2
5. Redon C., Pilch D., Rogakou E.,,at al (2002). "Histone H2A variants H2AX and H2AZ". Current Opinion in Genetics & Development. 12 (2), 162-169. 10.1016/S0959-437X(02)00282-4. PMID 11893489.16.
6. Enaki N.A., Paslari T., Bazgan S., at al.(2022) UVC radiation intensity dependence of pathogen decontamination rate: semiclassical theory and experiment. Eur Phys J Plus. 137(9):1047. 10.1140/epjp/s13360-022-03252-y. Epub 2022 PMID: 36123970; PMCID: PMC9476412.
7. Enaki, N.A., Munteanu, I., Paslari, T., at al. (2023) Topological Avenue for Efficient Decontamination of Large Volumes of Fluids via UVC Irradiation of Packed Metamaterials. Materials 2023, 16, 4559. https://doi.org/10.3390/ma16134559
8. Munteanu I., Turcan M., Starodub E., at al. (2022) Ultraviolet C Radiation for Disinfection and Protection Using Periodical Optical Structure for Dental Implant. ˆIn: IEEE Xplore, 2023. EHealth and Bioengineering Conference (EHB), 17-18 November Iasi, Romania , p. 1-4 . 10.1109/EHB55594.2022.9991449.
9. Enaki N., Paslari T., Bazgan S., at al. (2022) The efficiency of Screw channels in metamaterials for pathogen decontamination under ultraviolet C radiation. In: International Journal of Medical Science and Clinical Invention, 2022, nr. 6(9), pp. 6153-6156. ISSN -. 10.18535/ijmsci/v9i06.05 21.
10. Munteanu I., Starodub E., Bazgan S., at al,(2024) Ultraviolet C intensity dependence of decontamination efficiency for pathogens as function of repacked metamaterials with screw channels. Eur Biophys J. 53(3), 133-145. 10.1007/s00249-024-01702-2
11. Lans H. H., Hoeijmakers J.H.J., Vermeulen W., at al. (2019) The DNA damage response to transcription stress Nat. Rev. Mol. Cell Biol., 20, 766-784,
12. Marteijn J.A., Lans H., Vermeulen W., at al. (2014) Understanding nucleotide excision repair and its roles in cancer and ageing Nat. Rev. Mol. Cell Biol., 15, 465-481, 10.1038/nrm3822
13. Pinak M. (2006) Enzymatic recognition of radiation-produced oxidative DNA lesion. In the book: Molecular dynamics approach in Modern Methods for Theoretical Physical Chemistry of Biopolymers", Edited by: Evgeni B. Starikov, James P. Lewis and Shigenori Tanaka, lsevier, 10,

191-210.
14. Li X., Luk H. K. H. (2019) Human Corona viruses: General Features. In: Reference Module in Biomedical Sciences. Amsterdam: Elsevier; 1-6, 10.1016/B978-0-12- 801238-3.95704-0
15. Khailany R. A., Safdar M., Ozaslanc M. (2020) Genomic characterization of a novel SARS-CoV-2. Gene Rep. 19, 100682, 10.1016/j.genrep.2020.100682
16. Sarasin A. R., Hanawalt P.C. (1980) Replication of ultraviolet-irradiated simian virus 40 in monkey kidney cells. Journal of molecular biology. 138(2) , 299-319.
17. Schreier W. J., Schrader W. J., Koller F. O., at al.(2007) Thymine Dimerization in DNA is an Ultrafast Photoreaction, Science. 315, 625-629, 10.1126/science.1135428.
18. Born M., Oppenheimer J. R. (1927)" Zur Quantentheorie der Molekeln" [On the Quantum Theory of Molecules]. Annalen der Physik (in German). 389(20) 457?484. Bibcode:1927AnP...389.457B. 10.1002/andp.19273892002.
19. Loudon R. (2000) The Quantum Theory of Light. (Oxford, 2000) 448.
20. Rastogi R.P., Kumar R. A., Tyagi M. B., at al. (2010) Molecular Mechanisms of Ultraviolet Radiation.
21. Induced DNA Damage and Repair, SAGE-Hindawi Access to Research Journal of Nucleic Acids Article ID 592980, 10.4061/2010/592980
22. Jaiswal V. K., Segarra-Marti J., Marazzi M., at al (2020) First-principles characterization of the singlet excited state manifold in DNA/RNA nucleobases, Phys. Chem. Chem. Phys., 22, 15496-15508, DOI https://doi.org/10.1039/D0CP01823F
23. Duan H.G., Prokhorenko V. I., Cogdell R. J., at al. (2017) Nature does not rely on long-lived electronic quantum coherence for photosynthetic energy transfer, Proceedings of the National Academy of Sciences, 114 (32), 8493-8498, 10.1073/pnas.1702261114
24. Harush E. Z., Dubi Y. (2021) Do photosynthetic complexes use quantum coherence to increase their efficiency? Probably not, Sci Advv.7(8), FebPMC7888942; 10.1126/sciadv.abc4631
25. Baker N. R. (2000) Chlorophyll fluorescence: a probe of photosynthesis in vivo. Annu Rev Plant Biol. 59, 89-113; 10.1146/annurev.arplant.59.032607.092759. PMID: 18444897.
26. Yong E (2012) Yeast suggests speedy start for multicellular life. Nature News Springer Nature jan 16. 10.1038/nature.2012.9810.S2CID 84392827.
27. Enaki N.A. (2024) Cooperative properties of multiple quantum scattering: I quantum nutation. Phys Scripta. 99(4), 045102. 10.1088/1402-4896/ad29cb
28. Enaki N.A.(2024) Cooperative properties of multiple quantum scattering: II. Coherentlasing. Phys Scripta. 2024, 99(4), 045101. 1088/1402-4896/ad2ac0
29. Enaki N.A. (2021), Mutual cooperative effects between the mode components of two-photon and Raman induced cavity lasing processes. Opt Commun., 498, 127124. 10.1016/j.optcom.2021.127124
30. Mandal R., Mohammadi X., Wiktor A. at al. (2020) Applications of pulsed light decontamination technology in food processing: An overview, Appl. Sci. 10, 3606. https://doi.org/10.3390/app10103606
31. Jean J., Rodriguez-Lopez M.I., Jubinville E. at al.(2021) Potential of pulsed light technology for control of SARS-CoV-2 in hospital environments, Journal of Photochemistry and Photobiology B:
32. Biology 215, 112106. https://doi.org/10.1016/j.jphotobiol.2020.112106